Journal of Thermal Stresses
Publication details, including instructions for authors and subscription information:
http://www.informaworld.com/smpp/title~content=t713723680

An Efficient Semi-Analytical Model for Composite and Sandwich Plates Subjected to Thermal Load

Tarun Kant [a]; Sandeep S. Pendhari [a]; Yogesh M. Desai [a]
[a] Department of Civil Engineering, Indian Institute of Technology Bombay, Powai, Mumbai, India

Online Publication Date: 01 January 2008
To cite this Article: Kant, Tarun, Pendhari, Sandeep S. and Desai, Yogesh M. (2008) 'An Efficient Semi-Analytical Model for Composite and Sandwich Plates Subjected to Thermal Load', Journal of Thermal Stresses, 31:1, 77 - 103
To link to this article: DOI: 10.1080/01495730701738264
URL: http://dx.doi.org/10.1080/01495730701738264

Journal of Thermal Stresses, 31: 77–103, 2008

ISSN: 0149-5739 print/1521-074X online
DOI: 10.1080/01495730701738264

AN EFFICIENT SEMI-ANALYTICAL MODEL FOR COMPOSITE AND SANDWICH PLATES SUBJECTED TO THERMAL LOAD

Tarun Kant, Sandeep S. Pendhari, and Yogesh M. Desai
Department of Civil Engineering, Indian Institute of Technology Bombay, Powai, Mumbai, India

A simple, semi-analytical model with mixed (stresses and displacements) fundamental variables starting from the exact three dimensional (3D) governing partial differential equations (PDEs) of laminated composite and sandwich plates for thermo-mechanical stress analysis has been presented in this paper. The plate is assumed simply supported on all four edges. Two different temperature variations through the thickness of plates are considered for numerical investigation. The accuracy and the effectiveness of the proposed model are assessed by comparing numerical results from the present investigation with the available elasticity solutions. Some new results for sandwich laminates are also presented for future reference.

Keywords: Composites; Laminates; Sandwich; Semi-analytical; Thermal load

INTRODUCTION

Laminated composite and sandwich plates are extensively used due to their high specific strength and high specific stiffness. With the advancement of the technology of laminated materials, it is now possible to use these materials in high temperature situations. However, composites have no yield-limit, unlike metals and have a variety of failure modes, such as fiber failure, matrix cracking, inter fiber failure and delamination, which give rise to a damage growing in service. Moreover, composite and sandwich plates are subjected to significant thermal stresses due to different thermal properties of the adjacent laminas and therefore accurate predictions of thermally induced deformations and stresses represent a major concern in design of conventional structures.

Behavior of composite and sandwich plates can be characterized by a complex 3D state of stress. In many instances, these laminated structural elements are moderately thick in relation to their span dimensions. For thick or moderately thick structural elements, the normal to the mid surface is distorted due to inhomogeneity in the transverse shear moduli, which is smaller than in-plane Young's moduli,

Received 30 April 2007; accepted 11 August 2007.

Partial support of USIF Indo-US Collaborative Sponsored Research Project IND104 (95IU001) is gratefully acknowledged. Suggestions of the reviewers, which have been incorporated in the final version of the paper, are very much appreciated.

Address correspondence to Tarun Kant, Department of Civil Engineering, Indian Institute of Technology Bombay, Powai, Mumbai 400 076, India. E-mail: tkant@civil.iitb.ac.in

resulting in significant effects of transverse shear deformation and also transverse normal deformation.

The 3D elasticity analysis of laminates with a large number of orthotropic/isotropic layers becomes very complex [1–3]. Therefore, researchers have their attention on two dimensional (2D) analytical models by introducing some assumptions concerning the deformation of the transverse normals that are dependent on the nature of problem under consideration.

Classical lamination plate theory (CLPT) is based on the main assumption that the laminate is thin. As a consequence it is assumed that the normal to the laminate mid surface remains straight, inextensible and normal during the deformation. Maulbetsch [4] seems to have written the first paper, available in the literature, on thermal stresses in isotropic plates and Pell [5] is the first who studied thermal deflections of anisotropic thin plates under arbitrary temperature loading. On the other hand, the first-order shear deformation theory (FOST), based on Reissner [6] and Mindlin [7] approaches, considers effects of the transverse shear deformation by assuming it to be constant through the thickness of laminates, has been used by Reddy and Chao [8], Weinstein et al. [9], Rolfes et al. [10] and Argyris and Tenek [11]. Due to the constant shear assumption, FOST is inadequate to account for accurate shear distortion and a fictitious shear correction coefficient to correct the shear strain energy is normally used. Further, several higher-order shear deformation theories (HOSTs) with Taylor series-type expansion in the thickness direction for the displacements have been developed for composite and sandwich plates under thermal loading [12–14].

CLPT, FOST and HOST are the equivalent single layer (ESL) theories in which slope discontinuity in the inplane displacements and shear stress continuity at the laminae interfaces are not satisfied. To overcome the discrepancy of ESL, discrete layer theories (DLTs) and zig-zag theories have been developed for thermomechanical analysis of composite and sandwich plates [15, 16].

The present article which starts from 3D equations and does not make any kinetic or kinematic assumptions is mainly concerned with the formulation of a two-point boundary value problem (BVP) governed by a set of coupled first-order ODEs,

$$\frac{\mathrm{d}}{\mathrm{d}z}\mathbf{y}(z) = \mathbf{A}(z)\mathbf{y}(z) + \mathbf{p}(z) \tag{1}$$

in the interval $-h/2 \leq z \leq h/2$ with any half of the dependent variables prescribed at the edges $z = \pm h/2$ under thermal loading. Here, $\mathbf{y}(z)$ is an n-dimensional vector of fundamental variables whose number (n) equals the order of PDE, $\mathbf{A}(z)$ is a $n \times n$ coefficient matrix (which is a function of material properties in the thickness direction) and $\mathbf{p}(z)$ is an n-dimensional vector of non-homogenous (loading) terms. It is clearly seen that mixed and/or non-homogeneous boundary conditions are easily admitted in this formulation.

THEORETICAL FORMULATION

A plate composed of a number of isotropic/orthotropic, linear elastic laminae of uniform thickness with plan dimension $a \times b$ and thickness 'h' is considered (Figure 1). The angle between the fiber direction and reference axis, x is measured

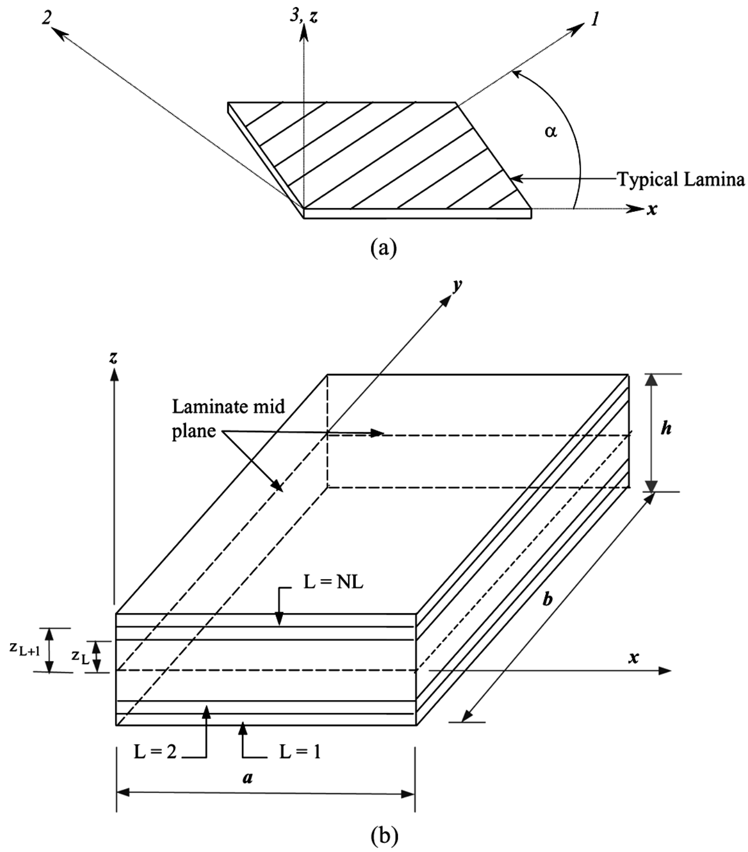

Figure 1 Laminate geometry with positive set of lamina/laminate reference axes and fiber orientation.

in anticlockwise direction as shown in Figure 1. Simply (diaphragm) supported end conditions on all four edges are considered (Table 1). Plate is subjected to only thermal load and all surfaces are free from any external stresses. Further, it is assumed that the thermal load is distributed linearly through the thickness (Figure 2).

$$\Delta T(x, y, z) = T_0(x, y) + \frac{2z}{h} T_1(x, y) \tag{2}$$

Constitute Relations

Each lamina in the laminate has been considered to be in a 3D state of stress so that the constitutive relation for a typical ith lamina with reference to the principal material coordinate axes (1, 2 and 3) can be written as,

$$(\varepsilon_1)^i = \left(\frac{1}{E_1}\sigma_1 - \frac{\nu_{21}}{E_2}\sigma_2 - \frac{\nu_{31}}{E_3}\sigma_3 + \alpha_{t1} T \right)^i$$

Table 1 Boundary conditions (BCs)

	BC imposed on displacement field	BC imposed on stress field
Face $x = 0,\ a$	$v = w = 0$	—
Face $x = a/2$	$u = 0$	$\tau_{xz} = 0$
Face $y = 0,\ b$	$u = w = 0$	—
Face $y = b/2$	$v = 0$	$\tau_{yz} = 0$
Top face $z = h/2$	—	$\tau_{xz} = \tau_{yz} = 0$ and $\sigma_z = 0$
Bottom face $z = -h/2$	—	$\tau_{xz} = \tau_{yz} = \sigma_z = 0$

$$(\varepsilon_2)^i = \left(-\frac{\nu_{12}}{E_1}\sigma_1 + \frac{1}{E_2}\sigma_2 - \frac{\nu_{32}}{E_3}\sigma_3 + \alpha_{t2}T\right)^i$$

$$(\varepsilon_3)^i = \left(-\frac{\nu_{13}}{E_1}\sigma_1 - \frac{\nu_{23}}{E_2}\sigma_2 + \frac{1}{E_3}\sigma_3 + \alpha_{t3}T\right)^i \tag{3}$$

$$(\gamma_{12})^i = \left(\frac{\tau_{12}}{G_{12}}\right)^i \quad (\gamma_{13})^i = \left(\frac{\tau_{13}}{G_{13}}\right)^i \quad \text{and} \quad (\gamma_{23})^i = \left(\frac{\tau_{23}}{G_{23}}\right)^i$$

in which $\alpha_{t1}T$, $\alpha_{t2}T$, and $\alpha_{t3}T$ are the free thermal strains that arise due to temperature variation. These can also be written as,

$$\begin{Bmatrix} \sigma_1 \\ \sigma_2 \\ \sigma_3 \\ \tau_{12} \\ \tau_{13} \\ \tau_{23} \end{Bmatrix}^i = \begin{bmatrix} C_{11} & C_{12} & C_{13} & 0 & 0 & 0 \\ & C_{22} & C_{23} & 0 & 0 & 0 \\ & & C_{33} & 0 & 0 & 0 \\ & & & C_{44} & 0 & 0 \\ & Sym. & & & C_{55} & 0 \\ & & & & & C_{66} \end{bmatrix}^i \begin{Bmatrix} \varepsilon_1 - \alpha_{t1}T \\ \varepsilon_2 - \alpha_{t2}T \\ \varepsilon_3 - \alpha_{t3}T \\ \gamma_{12} \\ \gamma_{13} \\ \gamma_{23} \end{Bmatrix}^i \tag{4}$$

where σ_1, σ_2, σ_3, τ_{12}, τ_{13}, τ_{23} are stresses and ε_1, ε_2, ε_3, γ_{12}, γ_{13}, γ_{23} are linear strain components with reference to the lamina coordinates 1, 2, and 3. C_{mn}'s

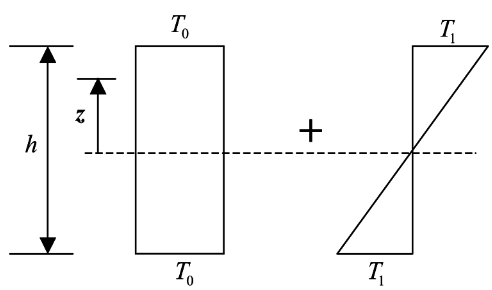

$$\Delta T(x,y,z) = T_0(x,y) + \frac{2z}{h}T_1(x,y)$$

Figure 2 Through thickness temperature distribution.

$(m, n = 1, \ldots, 6)$ are elasticity constants of the ith lamina with reference to the fiber axes $(1, 2, 3)$ defined in Appendix A. Stress-strain relations for the ith lamina in laminate coordinates (x, y, z) can be written as,

$$\begin{Bmatrix} \sigma_x \\ \sigma_y \\ \sigma_z \\ \tau_{xy} \\ \tau_{xz} \\ \tau_{yz} \end{Bmatrix} = \begin{bmatrix} Q_{11} & Q_{12} & Q_{13} & Q_{14} & 0 & 0 \\ & Q_{22} & Q_{23} & Q_{24} & 0 & 0 \\ & & Q_{33} & Q_{34} & 0 & 0 \\ & & & Q_{44} & 0 & 0 \\ & Sym. & & & Q_{55} & Q_{56} \\ & & & & & Q_{66} \end{bmatrix} \begin{Bmatrix} \varepsilon_x - \alpha_{tx} T \\ \varepsilon_y - \alpha_{ty} T \\ \varepsilon_z - \alpha_{tz} T \\ \gamma_{xy} - \alpha_{txy} T \\ \gamma_{xz} \\ \gamma_{yz} \end{Bmatrix} \tag{5}$$

where $\sigma_x, \sigma_y, \sigma_z, \tau_{xy}, \tau_{xz}, \tau_{yz}$ are stresses; $\varepsilon_x, \varepsilon_y, \varepsilon_z, \gamma_{xy}, \gamma_{xz}, \gamma_{yz}$ are strain components and $\alpha_{tx}T$, $\alpha_{ty}T$, $\alpha_{tz}T$, $\alpha_{txy}T$ are free thermal strains with respect to laminate axes (x, y, z) and Q_{mn}'s $(m, n = 1, \ldots, 6)$ are the transformed elasticity constants of the ith lamina with reference to the laminate axes. Elements of matrix $[Q]$ are defined in Appendix B.

Strain-Displacement Relationship

General 3D linear strain-displacement relations can be written as,

$$\begin{gathered} \varepsilon_x = \frac{\partial u}{\partial x} \quad \varepsilon_y = \frac{\partial v}{\partial y} \quad \varepsilon_z = \frac{\partial w}{\partial z} \\ \gamma_{xy} = \frac{\partial u}{\partial y} + \frac{\partial v}{\partial x} \quad \gamma_{xz} = \frac{\partial u}{\partial z} + \frac{\partial w}{\partial x} \quad \gamma_{yz} = \frac{\partial v}{\partial z} + \frac{\partial w}{\partial y} \end{gathered} \tag{6}$$

Equations of Equilibrium

The 3D differential equations of equilibrium are,

$$\begin{gathered} \frac{\partial \sigma_x}{\partial x} + \frac{\partial \tau_{yx}}{\partial y} + \frac{\partial \tau_{zx}}{\partial z} + B_x = 0 \\ \frac{\partial \tau_{xy}}{\partial x} + \frac{\partial \sigma_y}{\partial y} + \frac{\partial \tau_{zy}}{\partial z} + B_y = 0 \\ \frac{\partial \tau_{xz}}{\partial x} + \frac{\partial \tau_{yz}}{\partial y} + \frac{\partial \sigma_z}{\partial z} + B_z = 0 \end{gathered} \tag{7}$$

Here, B_x, B_y and B_z are components of body force in x, y and z directions, respectively.

Partial Differential Equations

Equations (5)–(7) have a total of 15 unknowns, six stresses $(\sigma_x, \sigma_y, \sigma_z, \tau_{xy}, \tau_{xz}, \tau_{yz})$, 6 strains $(\varepsilon_x, \varepsilon_y, \varepsilon_z, \gamma_{xy}, \gamma_{xz}, \gamma_{yz})$ and 3 displacements (u, v, w) in 15 equations. After simple algebraic manipulations, a system of PDEs involving only 6 fundamental variables $u, v, w, \tau_{xz}, \tau_{yz}$ and σ_z called "primary variables" are obtained as follows:

$$
\begin{aligned}
\frac{\partial u}{\partial z} &= \frac{1}{(Q_{55}Q_{66} - Q_{56}Q_{65})}\left[-Q_{65}\tau_{yz} + Q_{66}\tau_{xz}\right] - \frac{\partial w}{\partial x} \\
\frac{\partial v}{\partial z} &= \frac{1}{(Q_{55}Q_{66} - Q_{56}Q_{65})}\left[Q_{55}\tau_{yz} - Q_{56}\tau_{xz}\right] - \frac{\partial w}{\partial y} \\
\frac{\partial w}{\partial z} &= \frac{1}{Q_{33}}\left[\sigma_z - Q_{31}\frac{\partial u}{\partial x} - Q_{34}\frac{\partial u}{\partial y} - Q_{32}\frac{\partial v}{\partial y} - Q_{34}\frac{\partial v}{\partial x}\right] \\
&\quad + \frac{T}{Q_{33}}\left(Q_{31}\alpha_{tx} + Q_{32}\alpha_{ty} + Q_{33}\alpha_{tz} + Q_{34}\alpha_{txy}\right) \\
\frac{\partial \tau_{xz}}{\partial z} &= \left(-Q_{11} + \frac{Q_{13}Q_{31}}{Q_{33}}\right)\frac{\partial^2 u}{\partial x^2} + \left(-Q_{41} - Q_{14} + \frac{Q_{13}Q_{34}}{Q_{33}} + \frac{Q_{43}Q_{31}}{Q_{33}}\right)\frac{\partial^2 u}{\partial x \partial y} \\
&\quad + \left(-Q_{44} + \frac{Q_{43}Q_{34}}{Q_{33}}\right)\frac{\partial^2 u}{\partial y^2} + \left(-Q_{14} + \frac{Q_{13}Q_{34}}{Q_{33}}\right)\frac{\partial^2 v}{\partial x^2} \\
&\quad + \left(-Q_{12} - Q_{44} + \frac{Q_{13}Q_{32}}{Q_{33}} + \frac{Q_{43}Q_{34}}{Q_{33}}\right)\frac{\partial^2 v}{\partial x \partial y} \\
&\quad + \left(-Q_{42} + \frac{Q_{43}Q_{32}}{Q_{33}}\right)\frac{\partial^2 v}{\partial y^2} - \left(\frac{Q_{13}}{Q_{33}}\right)\frac{\partial \sigma_z}{\partial x} - \left(\frac{Q_{43}}{Q_{33}}\right)\frac{\partial \sigma_z}{\partial y} - B_x \\
&\quad - \left[\left(-Q_{11} + \frac{Q_{13}Q_{31}}{Q_{33}}\right)\alpha_{tx} + \left(-Q_{12} + \frac{Q_{13}Q_{32}}{Q_{33}}\right)\alpha_{ty} + \left(-Q_{14} + \frac{Q_{13}Q_{34}}{Q_{33}}\right)\alpha_{txy}\right]\frac{\partial T}{\partial x} \\
&\quad - \left[\left(-Q_{41} + \frac{Q_{43}Q_{31}}{Q_{33}}\right)\alpha_{tx} + \left(-Q_{42} + \frac{Q_{43}Q_{32}}{Q_{33}}\right)\alpha_{ty} + \left(-Q_{44} + \frac{Q_{43}Q_{34}}{Q_{33}}\right)\alpha_{txy}\right]\frac{\partial T}{\partial y} \\
\frac{\partial \tau_{yz}}{\partial z} &= \left(-Q_{41} + \frac{Q_{43}Q_{31}}{Q_{33}}\right)\frac{\partial^2 u}{\partial x^2} + \left(-Q_{21} - Q_{44} + \frac{Q_{23}Q_{31}}{Q_{33}} + \frac{Q_{43}Q_{34}}{Q_{33}}\right)\frac{\partial^2 u}{\partial x \partial y} \\
&\quad + \left(-Q_{24} + \frac{Q_{23}Q_{34}}{Q_{33}}\right)\frac{\partial^2 u}{\partial y^2} + \left(-Q_{44} + \frac{Q_{43}Q_{34}}{Q_{33}}\right)\frac{\partial^2 v}{\partial x^2} \\
&\quad + \left(-Q_{24} - Q_{42} + \frac{Q_{23}Q_{34}}{Q_{33}} + \frac{Q_{43}Q_{32}}{Q_{33}}\right)\frac{\partial^2 v}{\partial x \partial y} \\
&\quad + \left(-Q_{22} + \frac{Q_{23}Q_{32}}{Q_{33}}\right)\frac{\partial^2 v}{\partial y^2} - \left(\frac{Q_{43}}{Q_{33}}\right)\frac{\partial \sigma_z}{\partial x} - \left(\frac{Q_{23}}{Q_{33}}\right)\frac{\partial \sigma_z}{\partial y} - B_y \\
&\quad - \left[\left(-Q_{21} + \frac{Q_{23}Q_{31}}{Q_{33}}\right)\alpha_{tx} + \left(-Q_{22} + \frac{Q_{23}Q_{32}}{Q_{33}}\right)\alpha_{ty} + \left(-Q_{24} + \frac{Q_{23}Q_{34}}{Q_{33}}\right)\alpha_{txy}\right]\frac{\partial T}{\partial y} \\
&\quad - \left[\left(-Q_{41} + \frac{Q_{43}Q_{31}}{Q_{33}}\right)\alpha_{tx} + \left(-Q_{42} + \frac{Q_{43}Q_{32}}{Q_{33}}\right)\alpha_{ty} + \left(-Q_{44} + \frac{Q_{43}Q_{34}}{Q_{33}}\right)\alpha_{txy}\right]\frac{\partial T}{\partial x} \\
\frac{\partial \sigma_z}{\partial z} &= -\frac{\partial \tau_{xz}}{\partial x} - \frac{\partial \tau_{yz}}{\partial y} - B_z
\end{aligned}
\tag{8}
$$

Inplane Variation of Primary Variables

The above PDEs defined by Eq. (8) can be reduced to a coupled first-order ODEs by using a double Fourier trigonometric series for primary variables satisfying completely the simple (diaphragm) end conditions at all 4 edges, $x = 0$, a and $y = 0$, b, as follows:

$$\begin{aligned}
u(x, y, z) &= \sum_{mn} u_{mn}(z) \cos \frac{m\pi x}{a} \sin \frac{n\pi y}{b} \\
v(x, y, z) &= \sum_{mn} v_{mn}(z) \sin \frac{m\pi x}{a} \cos \frac{n\pi y}{b} \\
w(x, y, z) &= \sum_{mn} w_{mn}(z) \sin \frac{m\pi x}{a} \sin \frac{n\pi y}{b} \\
\tau_{xz}(x, y, z) &= \sum_{mn} \tau_{xzmn}(z) \cos \frac{m\pi x}{a} \sin \frac{n\pi y}{b} \\
\tau_{yz}(x, y, z) &= \sum_{mn} \tau_{yzmn}(z) \sin \frac{m\pi x}{a} \cos \frac{n\pi y}{b} \\
\sigma_{z}(x, y, z) &= \sum_{mn} \sigma_{zmn}(z) \sin \frac{m\pi x}{a} \sin \frac{n\pi y}{b}
\end{aligned} \tag{9}$$

in the above both m, n are 1, 3, 5, 7, ...

Further, temperature variations along the inplane directions are also expressed in sinusoidal form as

$$T(x, y, z) = \sum_{m'n'} T_{m'n'}(z) \sin \frac{m'\pi x}{a} \sin \frac{n'\pi x}{b} \tag{10}$$

in which both m', n' also assume integer values 1, 3, 5, 7, ...

Linear First-Order Ordinary Differential Equations (ODEs)

On substitution of Eqs. (9) and (10) in Eq. (8), the following 6 coupled first-order ODEs corresponding to each set of modal values m and n are obtained.

$$\frac{d}{dz}\left\{\begin{matrix} u_{mn}(z) \\ v_{mn}(z) \\ w_{mn}(z) \\ \tau_{xzmn}(z) \\ \tau_{yzmn}(z) \\ \sigma_{zmn}(z) \end{matrix}\right\} = \begin{bmatrix} 0 & 0 & B_{13} & B_{14} & 0 & 0 \\ 0 & 0 & B_{23} & 0 & B_{25} & 0 \\ B_{31} & B_{32} & 0 & 0 & 0 & B_{36} \\ B_{41} & B_{42} & 0 & 0 & 0 & B_{46} \\ B_{51} & B_{52} & 0 & 0 & 0 & B_{56} \\ 0 & 0 & 0 & B_{64} & B_{65} & 0 \end{bmatrix} \left\{\begin{matrix} u_{mn}(z) \\ v_{mn}(z) \\ w_{mn}(z) \\ \tau_{xzmn}(z) \\ \tau_{yzmn}(z) \\ \sigma_{zmn}(z) \end{matrix}\right\} + \left\{\begin{matrix} 0 \\ 0 \\ p_3 \\ p_4 \\ p_5 \\ p_6 \end{matrix}\right\}$$

which can be written in compact form as,

$$\frac{d}{dz}\mathbf{y}(z) = \mathbf{B}_{ij}(z)\mathbf{y}(z) + \mathbf{p}(z) \tag{11}$$

The elements of matrices $\mathbf{B}_{ij}(z)$ and vector $\mathbf{p}(z)$ are given in the Appendix C.

Table 2 Transformation of a BVP into IVPs

	Starting edge; $z = -h/2$						Final edge; $z = h/2$						
Intg.	u	v	w	τ_{xz}	τ_{yz}	σ_z	u	v	w	τ_{xz}	τ_{yz}	σ_z	Load term
1	0 (assumed)	0 (assumed)	0 (assumed)	0 (known)	0 (known)	0 (known)	Y_{11}	Y_{21}	Y_{31}	Y_{41}	Y_{51}	Y_{61}	Include
2	1 (unity)	0	0	0	0	0	Y_{12}	Y_{22}	Y_{32}	Y_{42}	Y_{52}	Y_{62}	Delete
3	0	1 (unity)	0	0	0	0	Y_{13}	Y_{23}	Y_{33}	Y_{43}	Y_{53}	Y_{63}	Delete
4	0	0	1 (unity)	0	0	0	Y_{14}	Y_{24}	Y_{34}	Y_{44}	Y_{54}	Y_{64}	Delete
Final	X_1	X_2	X_3	known	known	known	u_T	v_T	w_T	0	0	0	Include

Equation (11), defines the governing two-point BVP in ODEs through thickness of the laminate in the domain $-h/2 < z < h/2$ with stress components known at the top and bottom faces. The basic approach to the numerical integration of the BVP defined in Eq. (11) is to transform the given BVP into a set of IVPs—one non-homogeneous and $n/2$ homogeneous. The solution of BVP defined by Eq. (11) is then obtained by forming a linear combination of one non-homogeneous and $n/2$ homogeneous solutions so as to satisfy the boundary conditions at $z = h/2$ [17]. This gives rise to a system of $n/2$ linear algebraic equations, the solutions of which determines the unknown $n/2$ components, X_1, X_2 and X_3 (Table 2) at the starting edge $z = -h/2$. Then a final numerical integration of Eq. (11) produces the desired results. Availability of efficient, accurate and robust ODE numerical integrators for IVPs helps in computing reliable values of the primary variables through the thickness. Change in material properties are incorporated by changing coefficients of material matrix appropriately for each lamina.

Secondary Relations

Secondary variables, σ_x, σ_y and τ_{xy} can be expressed in terms of primary variables with the help of constitutive and strain-displacement relation as,

$$
\begin{aligned}
\sigma_x = {} & \left(\frac{Q_{13}Q_{31}}{Q_{33}} - Q_{11}\right)\sum_{mn} u_{mn}(z)\left(\frac{m\pi}{a}\right)\sin\frac{m\pi x}{a}\sin\frac{n\pi y}{b} \\
& + \left(\frac{Q_{13}Q_{32}}{Q_{33}} - Q_{12}\right)\sum_{mn} v_{mn}(z)\left(\frac{n\pi}{b}\right)\sin\frac{m\pi x}{a}\sin\frac{n\pi y}{b} \\
& + \left(Q_{14} - \frac{Q_{13}Q_{34}}{Q_{33}}\right)\sum_{mn} u_{mn}(z)\left(\frac{n\pi}{b}\right)\cos\frac{m\pi x}{a}\cos\frac{n\pi y}{b} \\
& + \left(Q_{14} - \frac{Q_{13}Q_{34}}{Q_{33}}\right)\sum_{mn} v_{mn}(z)\left(\frac{m\pi}{a}\right)\cos\frac{m\pi x}{a}\cos\frac{n\pi y}{b} \\
& + \left(\frac{Q_{13}}{Q_{33}}\right)\sum_{mn} \sigma_{zmn}(z)\sin\frac{m\pi x}{a}\sin\frac{m\pi y}{b} \\
& + \left\{\left(\frac{Q_{13}Q_{31}}{Q_{33}} - Q_{11}\right)\alpha_{tx} + \left(\frac{Q_{13}Q_{32}}{Q_{33}} - Q_{12}\right)\alpha_{ty} + \left(\frac{Q_{13}Q_{34}}{Q_{33}} - Q_{14}\right)\alpha_{xty}\right\} \\
& \times \sum_{m'n'} T(z)\sin\frac{m'\pi x}{a}\sin\frac{n'\pi y}{b}\,\ldots\ldots\ldots
\end{aligned}
\tag{12}
$$

$$
\begin{aligned}
\sigma_y = {} & \left(\frac{Q_{23}Q_{31}}{Q_{33}} - Q_{11}\right)\sum_{mn} u_{mn}(z)\left(\frac{m\pi}{a}\right)\sin\frac{m\pi x}{a}\sin\frac{n\pi y}{b} \\
& + \left(\frac{Q_{23}Q_{32}}{Q_{33}} - Q_{22}\right)\sum_{mn} v_{mn}(z)\left(\frac{n\pi}{b}\right)\sin\frac{m\pi x}{a}\sin\frac{n\pi y}{b} \\
& + \left(Q_{24} - \frac{Q_{23}Q_{34}}{Q_{33}}\right)\sum_{mn} u_{mn}(z)\left(\frac{n\pi}{b}\right)\cos\frac{m\pi x}{a}\cos\frac{n\pi y}{b}
\end{aligned}
$$

$$
\begin{aligned}
&+\left(Q_{24}-\frac{Q_{23}Q_{34}}{Q_{33}}\right)\sum_{mn} v_{mn}(z)\left(\frac{m\pi}{a}\right)\cos\frac{m\pi x}{a}\cos\frac{n\pi y}{b}\\
&+\left(\frac{Q_{23}}{Q_{33}}\right)\sum_{mn}\sigma_{zmn}(z)\sin\frac{m\pi x}{a}\sin\frac{m\pi y}{b}\\
&+\left\{\left(\frac{Q_{23}Q_{31}}{Q_{33}}-Q_{21}\right)\alpha_{tx}+\left(\frac{Q_{23}Q_{32}}{Q_{33}}-Q_{22}\right)\alpha_{ty}+\left(\frac{Q_{23}Q_{34}}{Q_{33}}-Q_{24}\right)\alpha_{xty}\right\}\\
&\times\sum_{m'n'}T(z)\sin\frac{m'\pi x}{a}\sin\frac{n'\pi y}{b}\,\ldots\ldots\ldots
\end{aligned}
\tag{13}
$$

$$
\begin{aligned}
\tau_{xy}=&\left(\frac{Q_{43}Q_{31}}{Q_{33}}-Q_{11}\right)\sum_{mn} u_{mn}(z)\left(\frac{m\pi}{a}\right)\sin\frac{m\pi x}{a}\sin\frac{n\pi y}{b}\\
&+\left(\frac{Q_{43}Q_{32}}{Q_{33}}-Q_{42}\right)\sum_{mn} v_{mn}(z)\left(\frac{n\pi}{b}\right)\sin\frac{m\pi x}{a}\sin\frac{n\pi y}{b}\\
&+\left(Q_{44}-\frac{Q_{43}Q_{34}}{Q_{33}}\right)\sum_{mn} u_{mn}(z)\left(\frac{n\pi}{b}\right)\cos\frac{m\pi x}{a}\cos\frac{n\pi y}{b}\\
&+\left(Q_{44}-\frac{Q_{43}Q_{34}}{Q_{33}}\right)\sum_{mn} v_{mn}(z)\left(\frac{m\pi}{a}\right)\cos\frac{m\pi x}{a}\cos\frac{n\pi y}{b}\\
&+\left(\frac{Q_{43}}{Q_{33}}\right)\sum_{mn}\sigma_{zmn}(z)\sin\frac{m\pi x}{a}\sin\frac{m\pi y}{b}\\
&+\left\{\left(\frac{Q_{43}Q_{31}}{Q_{33}}-Q_{41}\right)\alpha_{tx}+\left(\frac{Q_{43}Q_{32}}{Q_{33}}-Q_{42}\right)\alpha_{ty}+\left(\frac{Q_{43}Q_{34}}{Q_{33}}-Q_{44}\right)\alpha_{xty}\right\}\\
&\times\sum_{m'n'}T(z)\sin\frac{m'\pi x}{a}\sin\frac{n'\pi y}{b}\,\ldots\ldots\ldots
\end{aligned}
\tag{14}
$$

NUMERICAL INVESTIGATION

A computer code is developed by incorporating the present formulation in FORTRAN 90 for the analysis of composite and sandwich plates under thermal load. Numerical investigations on various examples have been performed including validation of the present semi-analytical formulation and solution of new problems. The 3D elasticity solution presented by Bhaskar et al. [3] and Rohwer et al. [14] and other analytical solutions available in the literature have been used for proper comparison of the obtained results. Material properties used here have been tabulated in Table 3.

Two thermal load cases are considered here for numerical studies.

1. Equal temperature rise of the bottom and the top surface of the plate with sinusoidal inplane variations: $\Delta T(x, y, \pm h/2) = T_0 \sin\frac{\pi x}{a}\sin\frac{\pi y}{b}$, (Case A).
2. Equal rise and fall of temperature of the top and bottom surface of the plate with sinusoidal inplane variations: $\Delta T(x, y, h/2) = -\Delta T(x, y, -h/2) = T_0 \sin\frac{\pi x}{a}\sin\frac{\pi y}{b}$, (Case B).

Table 3 Material properties

Set	Source	Property		
I	Rohwer et al. [14]	$E_1 = 150.0\,\text{GPa}$ $\nu_{12} = 0.30$ $G_{12} = 5.0\,\text{GPa}$ $\alpha_1 = 0.139\text{E-}6\,\text{k}^{-1}$	$E_2 = 10.0\,\text{GPa}$ $\nu_{13} = 0.30$ $G_{13} = 5.0\,\text{GPa}$ $\alpha_2 = 9.0\text{E-}6\,\text{k}^{-1}$	$E_3 = 10.0\,\text{GPa}$ $\nu_{23} = 0.30$ $G_{23} = 3.378\,\text{GPa}$ $\alpha_3 = 9.0\text{E-}6\,\text{k}^{-1}$
II	Bhaskar et al. [3]	$E_1 = 172.4\,\text{GPa}$ $\nu_{12} = 0.25$ $G_{12} = 3.45\,\text{GPa}$ $\alpha_1 = 1.0\,\text{k}^{-1}$	$E_2 = 6.89\,\text{GPa}$ $\nu_{13} = 0.25$ $G_{13} = 3.45\,\text{GPa}$ $\alpha_2 = 1125.0\,\text{k}^{-1}$	$E_3 = 6.89\,\text{GPa}$ $\nu_{23} = 0.25$ $G_{23} = 1.378\,\text{GPa}$ $\alpha_3 = 1125.0\,\text{k}^{-1}$
			Face Sheet	
III	Khare et al. [18]	$E_1 = 172.4\,\text{GPa}$ $\nu_{12} = 0.25$ $G_{12} = 3.45\,\text{GPa}$ $\alpha_1 = 0.1\text{E-}5\,\text{k}^{-1}$	$E_2 = 6.89\,\text{GPa}$ $\nu_{13} = 0.25$ $G_{13} = 3.45\,\text{GPa}$ $\alpha_2 = 2.0\text{E-}5\,\text{k}^{-1}$	$E_3 = 6.89\text{GPa}$ $\nu_{23} = 0.25$ $G_{23} = 1.378\,\text{GPa}$ $\alpha_3 = 0.1\text{E-}5\,\text{k}^{-1}$
			Core Sheet	
		$E_1 = 0.276\,\text{GPa}$ $\nu_{12} = 0.25$ $G_{12} = 0.1104\,\text{GPa}$ $\alpha_1 = 0.1\text{E-}6\,\text{k}^{-1}$	$E_2 = 0.276\,\text{GPa}$ $\nu_{31} = 0.25$ $G_{13} = 0.414\,\text{GPa}$ $\alpha_2 = 0.2\text{E-}5\,\text{k}^{-1}$	$E_3 = 3.450\,\text{GPa}$ $\nu_{32} = 0.25$ $G_{23} = 0.414\,\text{GPa}$ $\alpha_3 = 0.1\text{E-}6\,\text{k}^{-1}$

Following normalizations have been used in all examples considered here for the comparison of the results.

$$s = \frac{a}{h} \quad \overline{u}, \overline{v} = \frac{1}{h\alpha_1 T_0 s^3}(u; v) \quad \overline{w} = \frac{h^3 w}{\alpha_1 T_0 a^4} \quad \overline{\sigma_z} = \frac{\sigma_z}{E_2 \alpha_1 T_0}$$
$$\left(\overline{\sigma_x}; \overline{\sigma_y}; \overline{\tau_{xy}}\right) = \frac{1}{E_2 \alpha_1 T_0 s^2}\left(\sigma_x; \sigma_y; \tau_{xy}\right) \quad \left(\overline{\tau_{xz}}; \overline{\tau_{yz}}\right) = \frac{1}{E_2 \alpha_1 T_0 s}\left(\tau_{xz}; \tau_{yz}\right) \tag{15}$$

in which bar over the variable defines its normalized value.

A convergence study on number of steps required for numerical integration in the thickness direction of the laminate is performed first for all examples. It is observed in all examples that 20–30 steps are enough for converged solution. Details of the convergence studies are not presented here for the sake of brevity. Illustrative examples considered in the present work are discussed next.

Example 1

A homogeneous, orthotropic plate with simple support end conditions (Table 1) on all four edges and subjected to thermal load has been considered to study the effect of the temperature distribution and validate the present methodology. Material properties are presented in Table 3(I). The normalized maximum stresses ($\overline{\sigma_x}$, $\overline{\sigma_y}$, $\overline{\tau_{xy}}$, $\overline{\tau_{xz}}$, $\overline{\tau_{yz}}$) and transverse displacement ($\overline{w}$) for various aspect ratios ranging from thick to thin plate are presented in Table 4 for both type of thermal loads. Moreover, through thickness variations of transverse shear stress ($\overline{\tau_{xz}}$), transverse normal stress ($\overline{\sigma_z}$), in-plane normal stress ($\overline{\sigma_x}$) and transverse displacement ($\overline{w}$) for an aspect ratio of 5 are shown in Figures 3 and 4 for

Table 4 Maximum stresses ($\overline{\sigma_x}, \overline{\sigma_y}, \overline{\tau_{xy}}, \overline{\tau_{xz}}$ and $\overline{\tau_{yz}}$) and the transverse displacement ($\overline{w}$) of square homogeneous orthotropic plates under thermal load

Case A: $\Delta T(x, y, \pm h/2) = T_0 \sin\frac{\pi x}{a} \sin\frac{\pi y}{b}$							
s	Source	$\overline{\sigma_x}\left(\frac{a}{2}, \frac{b}{2}; \pm\frac{h}{2}\right)$	$\overline{\sigma_y}\left(\frac{a}{2}, \frac{b}{2}; \pm\frac{h}{6}\right)$	$10\overline{\tau_{xy}}\left(0, 0, \pm\frac{h}{2}\right)$	$10\overline{\tau_{xz}}\left(0, \frac{b}{2}, \pm 0.3h\right)$	$10^2\overline{\tau_{yz}}\left(\frac{a}{2}, 0, \pm 0.3h\right)$	$10^2\overline{w}\left(\frac{a}{2}, \frac{b}{2}, \pm\frac{h}{2}\right)$
4	Present analysis	0.4143	−0.7446	−0.9598	±3.7943	±6.2979	±6.0309
10	Present analysis	−0.1261	−0.2092	−0.2233	±0.2864	±0.4218	±0.3780
20	Present analysis	−0.0484	−0.0538	−0.0547	±0.0188	±0.0269	±0.0236
Case B: $\Delta T(x, y, h/2) = -\Delta T(x, y, -h/2) = T_0 \sin\frac{\pi x}{a} \sin\frac{\pi y}{b}$							
s	Source	$\overline{\sigma_x}\left(\frac{a}{2}, \frac{b}{2}; \pm\frac{h}{2}\right)$	$\overline{\sigma_y}\left(\frac{a}{2}, \frac{b}{2}; \pm\frac{h}{2}\right)$	$10\overline{\tau_{xy}}\left(0, 0, \pm\frac{h}{2}\right)$	$\overline{\tau_{xz}}\left(0, \frac{b}{2}, \pm 0.3h\right)$	$\overline{\tau_{yz}}\left(\frac{a}{2}, 0, \pm 0.3h\right)$	$10^2\overline{w}\left(\frac{a}{2}, \frac{b}{2}, \pm\frac{h}{2}\right)$
4	Present analysis	±2.0164	∓2.0538	∓3.5566	0.9239	−0.8616	9.0226
10	Present analysis	±0.4845	∓0.5638	∓0.6380	0.2565	−0.2517	1.4042
20	Present analysis	±0.1198	∓0.1448	∓0.1405	0.0660	−0.0657	0.2916

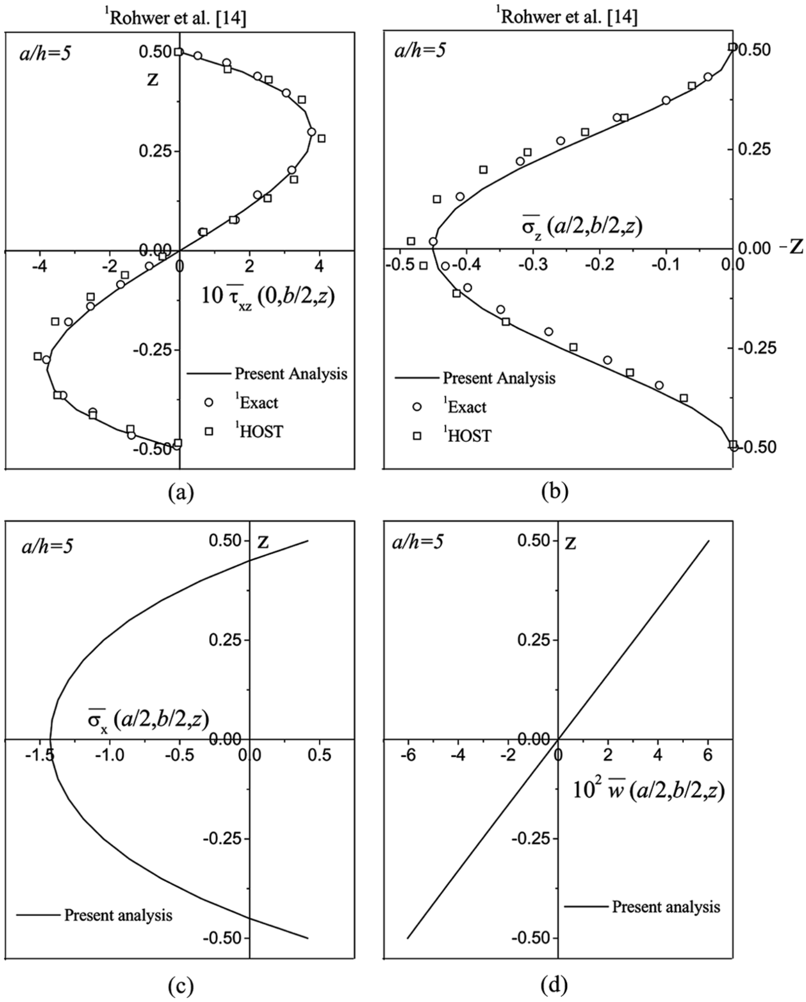

Figure 3 Variation of normalized (a) transverse shear stress $\overline{\tau_{xz}}$ (b) transverse normal stress $\overline{\sigma_z}$ (c) inplane normal stress $\overline{\sigma_x}$ (d) transverse displacement $\overline{w}$ through thickness of a homogeneous orthotropic plate subjected to thermal load, $\Delta T(x, y, \pm h/2) = T_0 \sin\frac{\pi x}{a} \sin\frac{\pi y}{b}$ (Case A).

case A and case B, respectively. 3D elasticity and HOST solutions given by Rohwer et al. [14] are also plotted on same trace for comparison of the present solution. This comparison clearly indicates that the present results are very close to the elasticity solutions compared to HOST and thus proves the superiority of the present model. Large value of $\overline{\tau_{xz}}$ as compared to $\overline{\tau_{yz}}$ (Table 4) is due to higher modulus values of G_{13} and E_1 as compared to G_{23} and E_2. Transverse normal stress ($\overline{\sigma_z}$) shows compression at the plate center (Figure 3b) and roughly cubic distribution of transverse shear stress ($\overline{\tau_{xz}}$) through the thickness of plate (Figure 3a) is observed for constant temperature (Case A). Moreover, in case B, the transverse normal stress ($\overline{\sigma_z}$) is found to be too small as compared to case A with compressive value in the

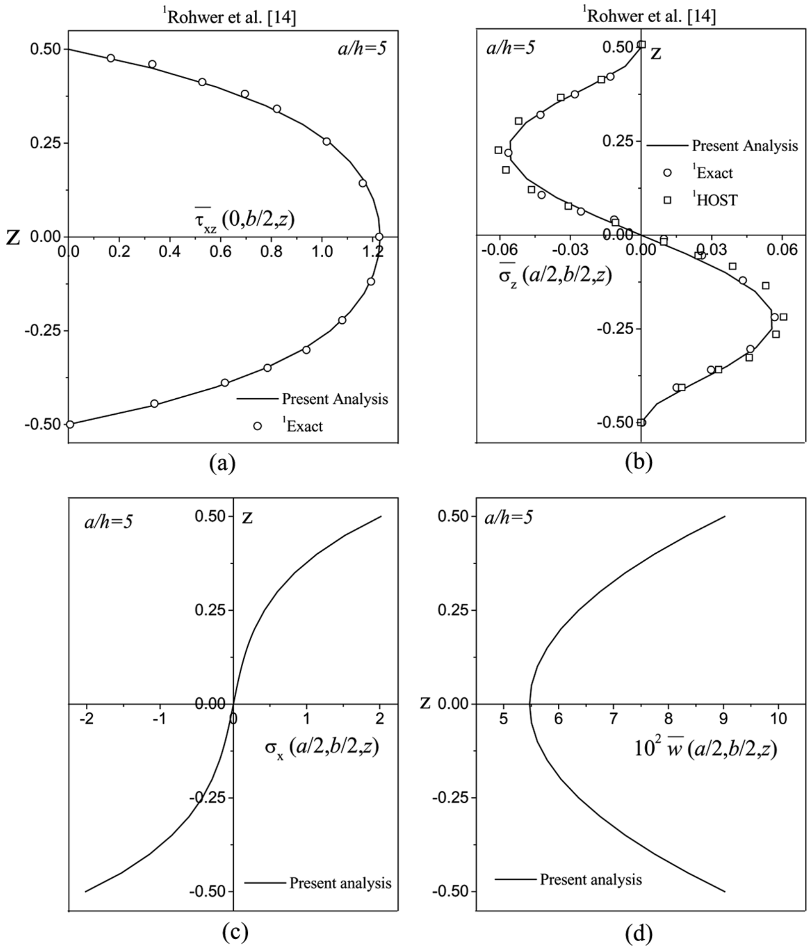

Figure 4 Variation of normalized (a) transverse shear stress $\overline{\tau_{xz}}$ (b) transverse normal stress $\overline{\sigma_z}$ (c) inplane normal stress $\overline{\sigma_x}$ (d) transverse displacement $\overline{w}$ through thickness of a homogeneous orthotropic plate subjected to thermal load, $\Delta T(x, y, h/2) = -\Delta T(x, y, -h/2) = T_0 \sin \frac{\pi x}{a} \sin \frac{\pi y}{b}$ (Case B).

upper half and tensile value in the lower half of plate. And transverse shear stresses $\overline{\tau_{xz}}$ and $\overline{\tau_{yz}}$ are found to be nearly same with opposite signs.

Example 2

Various three-layered, symmetric, cross-ply (0°/90°/0°), square laminates with aspect ratios, $s = 4$, 10 and 20 and simple support end conditions on all four edges (Table 1) subjected to constant (Case A) and varied (Case B) temperature distribution through thickness and sinusoidal variations along the inplane directions are considered here to show the ability of the present model to handle layered structure. Material properties are presented in Table 3(II). Results for aspect ratios, $s = 4$, 10 and 20 have been compared in Table 5 with elasticity solutions given by

Table 5 Maximum stresses ($\overline{\sigma_x}, \overline{\sigma_y}, \overline{\tau_{xy}}, \overline{\tau_{xz}}$ and $\overline{\tau_{yz}}$) and the transverse displacement ($\overline{w}$) of three layered symmetric (0°/90°/0°) square composite plates under thermal load

		Case A: $\Delta T(x, y, \pm h/2) = T_0 \sin \frac{\pi x}{a} \sin \frac{\pi y}{b}$					
s	Source	$\overline{\sigma_x}\left(\frac{a}{2}, \frac{b}{2}; \pm\frac{h}{2}\right)$	$\overline{\sigma_y}\left(\frac{a}{2}, \frac{b}{2}; \pm\frac{h}{6}\right)$	$\overline{\tau_{xy}}\left(0, 0, \pm\frac{h}{2}\right)$	$\overline{\tau_{xz}}\left(0, \frac{b}{2}, \pm 0.4h\right)$	$\overline{\tau_{yz}}\left(\frac{a}{2}, 0, \pm 0.4h\right)$	$10\overline{w}\left(\frac{a}{2}, \frac{b}{2}, \pm\frac{h}{2}\right)$
4	Present analysis	80.7516	−49.9119	−11.6824	±33.3088	∓51.0344	±26.5000
10	Present analysis	6.1090	−9.8927	−0.8247	±5.3374	∓9.8181	±0.6875
20	Present analysis	1.2300	−2.5547	−0.1614	±1.3334	∓2.5267	±0.0430
		Case B: $\Delta T(x, y, h/2) = -\Delta T(x, y, -h/2) = T_0 \sin \frac{\pi x}{a} \sin \frac{\pi y}{b}$					
s	Source	$\overline{\sigma_x}\left(\frac{a}{2}, \frac{b}{2}; \pm\frac{h}{2}\right)$	$\overline{\sigma_y}\left(\frac{a}{2}, \frac{b}{2}; \pm\frac{h}{2}\right)$	$\overline{\tau_{xy}}\left(0, 0, \pm\frac{h}{2}\right)$	$\overline{\tau_{xz}}\left(0, \frac{b}{2}, \pm 0.4h\right)$	$\overline{\tau_{yz}}\left(\frac{a}{2}, 0, \pm 0.4h\right)$	$\overline{w}\left(\frac{a}{2}, \frac{b}{2}, \pm\frac{h}{2}\right)$
4	Present analysis	±73.9496	∓53.5059	∓9.8113	21.2030	−32.1750	2.6679
	[1]Exact solution	±73.9375	∓53.5062	∓9.8113	21.2025	−32.1750	2.6680
10	Present analysis	±10.2630	∓10.1436	∓0.7629	6.0541	−6.6008	0.1739
	[1]Exact solution	±10.2600	∓10.1400	∓0.7629	6.0510	−6.6010	0.1739
20	Present analysis	±2.4550	∓2.6281	∓0.1437	1.6992	−1.7381	0.0303
	[1]Exact solution	±2.4550	∓2.6275	∓0.1438	1.6990	−1.7380	0.0303

[1]Bhaskar et al. [3].

Bhaskar et al. [3]. Present results are seen to be closest to the elasticity solutions. Through thickness variations of transverse shear stress ($\overline{\tau_{xz}}$), transverse normal stress ($\overline{\sigma_z}$), inplane normal stress ($\overline{\sigma_x}$) and inplane displacement ($\overline{u}$) for an aspect ratio of 5 have been presented in Figures 5 and 6 for case A and case B, respectively. Solutions are only available for varied temperature (Case B) and solutions with constant temperature (Case A) will be useful as benchmark solution in future. Variation of transverse shear stress ($\overline{\tau_{xz}}$) for constant temperature (Case A) is found to be smooth curved profile in the top and bottom lamina (0°) but almost linear profile is observed in the middle lamina (90°) with zero value at the mid-surface (Figure 5a), whereas for varied temperature (Case B), $\overline{\tau_{xz}}$ varies smoothly in curved fashion through the thickness (Figure 6a). Interesting distribution of transverse

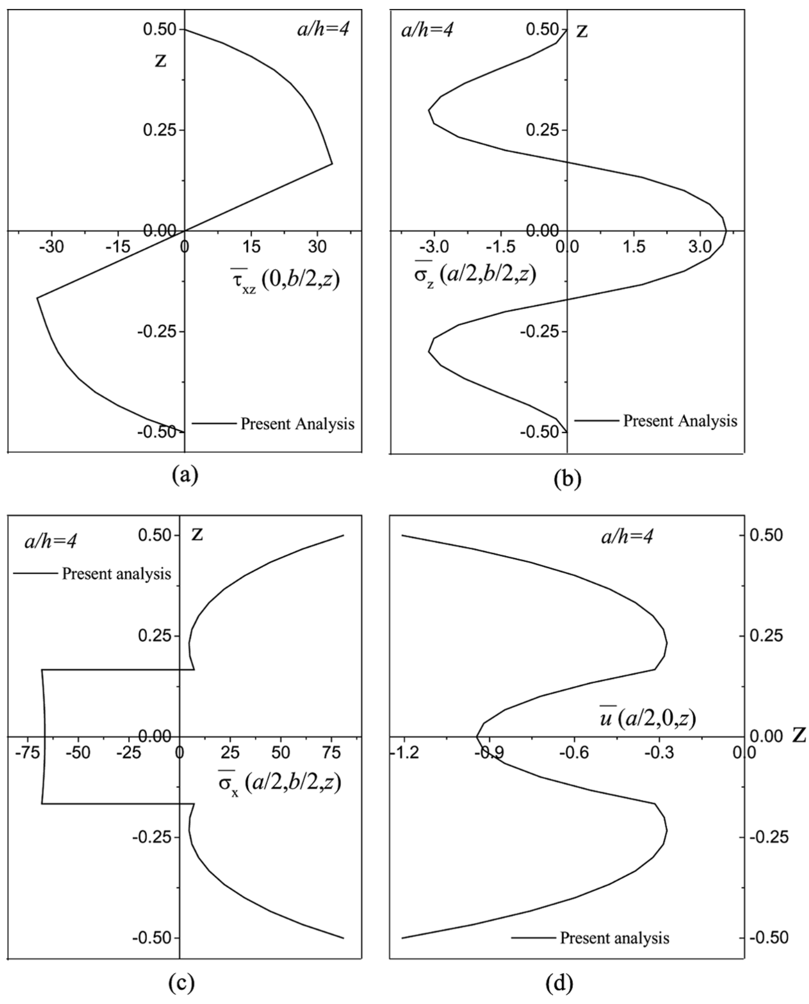

Figure 5 Variation of normalized (a) transverse shear stress $\overline{\tau_{xz}}$ (b) transverse normal stress $\overline{\sigma_z}$ (c) inplane normal stress $\overline{\sigma_x}$ (d) inplane displacement $\overline{u}$ through thickness of a 0°/90°/0° symmetric composite plate subjected to thermal load, $\Delta T(x, y, \pm h/2) = T_0 \sin \frac{\pi x}{a} \sin \frac{\pi y}{b}$ (Case A).

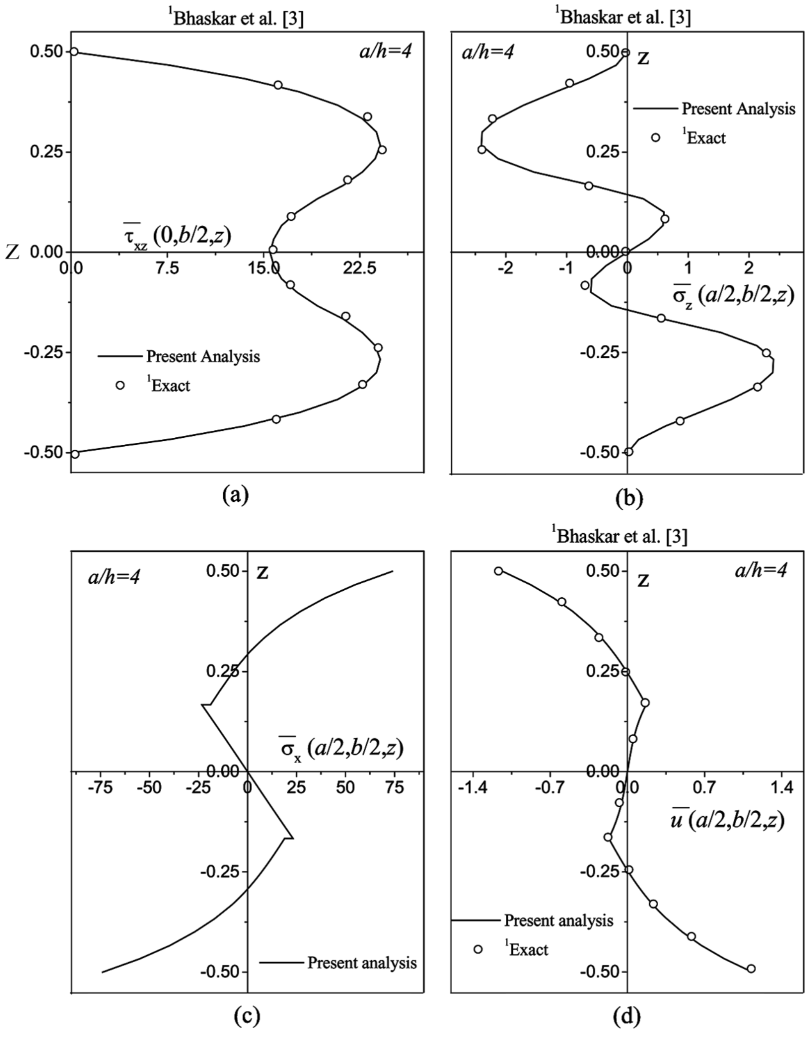

Figure 6 Variation of normalized (a) transverse shear stress $\overline{\tau_{xz}}$ (b) transverse normal stress $\overline{\sigma_z}$ (c) inplane normal stress $\overline{\sigma_x}$ (d) transverse displacement $\overline{w}$ through thickness of a 0°/90°/0° symmetric composite subjected to thermal load, $\Delta T(x, y, h/2) = -\Delta T(x, y, -h/2) = T_0 \sin \frac{\pi x}{a} \sin \frac{\pi y}{b}$ (Case B).

normal stress ($\overline{\sigma_z}$) is observed for this configuration in both types of loadings. In case of constant temperature (Case A), $\overline{\sigma_z}$ in top and bottom lamina (0°) shows compression whereas, $\overline{\sigma_z}$ in middle lamina (90°) shows tension at the plate center (Figure 5b) and in case of varied temperature (Case B), $\overline{\sigma_z}$ in top lamina (0°) is compressive, $\overline{\sigma_z}$ in bottom lamina (0°) is tensile and $\overline{\sigma_z}$ in middle lamina (90°) has mixed behavior of compression and tension below and above the mid-surface (Figure 6b) which proves the necessity of refined model to model the accurately such highly non-linear behaviour. All variations are observed to be symmetric about the mid-surface as expected.

Table 6 Maximum stresses ($\overline{\sigma_x}, \overline{\sigma_y}, \overline{\tau_{xy}}, \overline{\tau_{xz}}$ and $\overline{\tau_{yz}}$) and the transverse displacement ($\overline{w}$) of four layered unsymmetric (0°/90°/0°/90°) square composite plates under thermal load

Case A: $\Delta T(x, y, \pm h/2) = T_0 \sin \frac{\pi x}{a} \sin \frac{\pi y}{b}$											
s	Source	$\overline{\sigma_x}\left(\frac{a}{2}, \frac{b}{2}; \pm\frac{h}{2}\right)$		$\overline{\sigma_y}\left(\frac{a}{2}, \frac{b}{2}; \pm\frac{h}{6}\right)$		$10\overline{\tau_{xy}}\left(0, 0, \pm\frac{h}{2}\right)$	$\overline{\tau_{xz}}\left(0, \frac{b}{2}, \pm 0.25h\right)$		$\overline{\tau_{yz}}\left(\frac{a}{2}, 0, \pm 0.25h\right)$		$10^2\overline{w}\left(\frac{a}{2}, \frac{b}{2}, \pm\frac{h}{2}\right)$
4	Present analysis	−2.0651	2.5527	2.5527	−2.0651	−3.6261	−1.4881	−1.5429	1.5429	1.4881	±7.2837
10	Present analysis	−0.5663	0.5127	0.5127	−0.5663	−0.6322	−0.4048	−0.4042	0.4042	0.4048	±0.4582
20	Present analysis	−0.1449	0.1214	0.1214	−0.1449	−0.1399	−0.1035	−0.1033	0.1033	0.1034	±0.0287
Case B: $\Delta T(x, y, h/2) = -\Delta T(x, y, -h/2) = T_0 \sin \frac{\pi x}{a} \sin \frac{\pi y}{b}$											
s	Source	$\overline{\sigma_x}\left(\frac{a}{2}, \frac{b}{2}; \pm\frac{h}{2}\right)$		$\overline{\sigma_y}\left(\frac{a}{2}, \frac{b}{2}; \pm\frac{h}{2}\right)$		$10\overline{\tau_{xy}}\left(0, 0, \pm\frac{h}{2}\right)$	$\overline{\tau_{xz}}\left(0, \frac{b}{2}, \pm 0.2h\right)$		$\overline{\tau_{yz}}\left(\frac{a}{2}, 0, \pm 0.2h\right)$		$10^2\overline{w}\left(\frac{a}{2}, \frac{b}{2}, \pm\frac{h}{2}\right)$
4	Present analysis	−2.1008	−1.6496	1.6496	2.1008	∓3.2408	−1.0726	0.6986	0.6986	−1.0726	8.9098
10	Present analysis	−0.5479	−0.3719	0.3719	0.5479	∓0.6894	−0.2818	0.1870	0.1870	−0.2818	1.5447
20	Present analysis	−0.1385	−0.0903	0.0903	0.1385	∓0.1643	−0.0714	0.0476	0.0476	−0.0714	0.3422

Example 3

A 4-layered, unsymmetric, cross-ply (0°/90°/0°/90°), square composite plate with equal thickness under the thermal load is considered in this example with simple support end conditions (Table 1). Material properties are presented in Table 3(I). Results of the maximum normalized stresses ($\overline{\sigma_x}, \overline{\sigma_y}, \overline{\tau_{xy}}, \overline{\tau_{xz}}, \overline{\tau_{yz}}$) and transverse displacement ($\overline{w}$) are presented in Table 6 for various aspect ratios and through thickness variations of transverse shear stress ($\overline{\tau_{xz}}$), transverse normal stress ($\overline{\sigma_z}$), inplane normal stress ($\overline{\sigma_x}$) and transverse displacement ($\overline{w}$) are depicted in

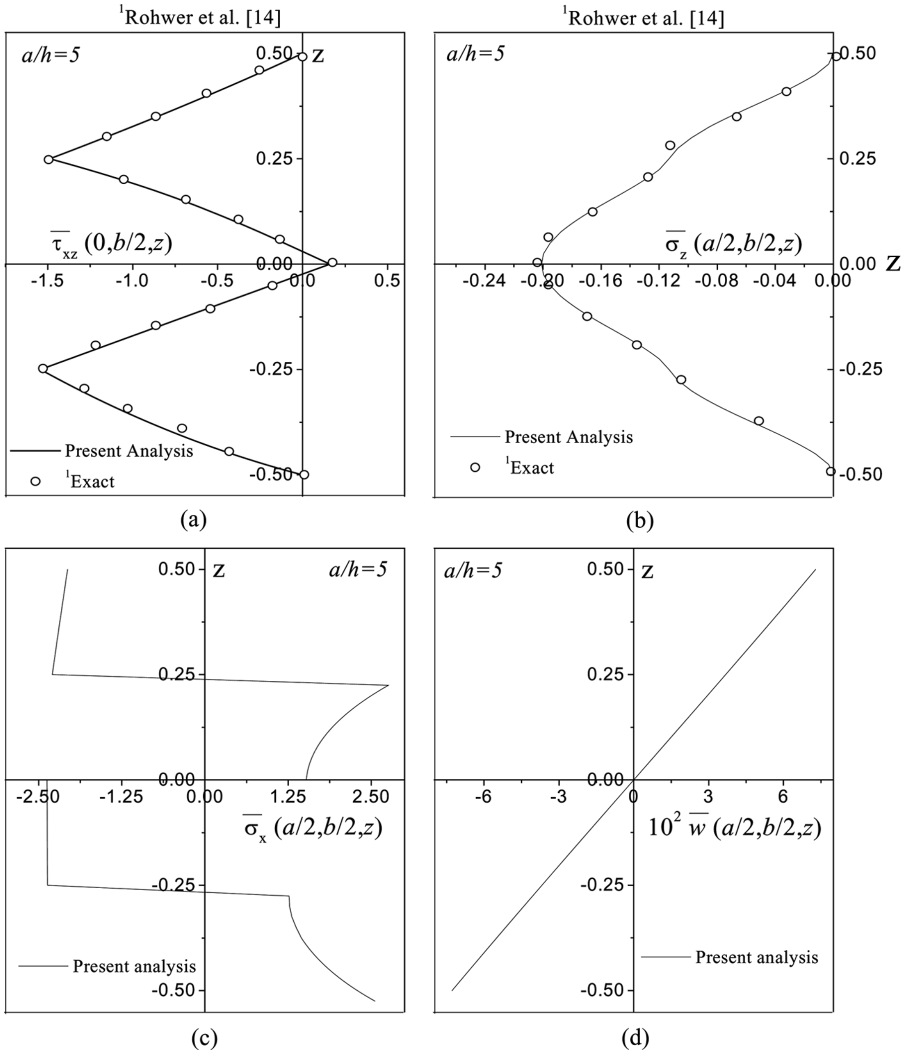

Figure 7 Variation of normalized (a) transverse shear stress $\overline{\tau_{xz}}$ (b) transverse normal stress $\overline{\sigma_z}$ (c) inplane normal stress $\overline{\sigma_x}$ (d) transverse displacement $\overline{w}$ through thickness of a 0°/90°/0°/90° unsymmetric composite plate subjected to thermal load, $\Delta T(x, y, \pm h/2) = T_0 \sin \frac{\pi x}{a} \sin \frac{\pi y}{b}$ (Case A).

Figures 7 and 8 for an aspect ratio of 5 for case A and case B, respectively. 3D elasticity solution given by Rohwer et al. [14] is used for comparison of the results obtained through present investigations. Excellent agreements of present results with elasticity solutions suggest that the formulation is capable to handle such unsymmetric laminate configurations. It is also seen that transverse shear stress $\overline{\tau_{xz}}$ has symmetry about mid plane with shear stress $\overline{\tau_{yz}}$ (Table 6). Zig-zag variation of transverse shear stress ($\overline{\tau_{xz}}$) through the thickness of plate is observed (Figure 7a and 8a) and this is due to the abrupt change in stiffness between 0° and 90° layers

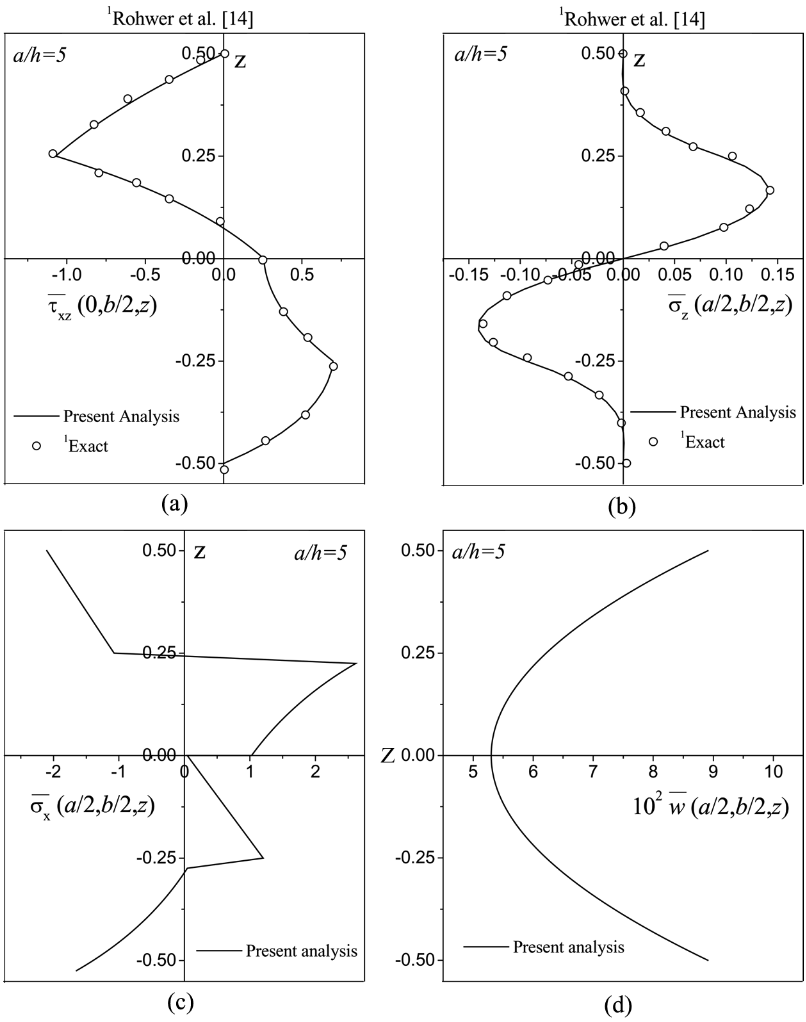

Figure 8 Variation of normalized (a) transverse shear stress $\overline{\tau_{xz}}$ (b) transverse normal stress $\overline{\sigma_z}$ (c) inplane normal stress $\overline{\sigma_x}$ (d) transverse displacement $\overline{w}$ through thickness of a 0°/90°/0°/90° unsymmetric composite subjected to thermal load, $\Delta T(x, y, h/2) = -\Delta T(x, y, -h/2) = T_0 \sin\frac{\pi x}{a}\sin\frac{\pi y}{b}$ (Case B).

Table 7 Maximum stresses ($\overline{\sigma_x}$, $\overline{\sigma_y}$, $\overline{\tau_{xy}}$, $\overline{\tau_{xz}}$ and $\overline{\tau_{yz}}$) and the transverse displacement ($\overline{w}$) of symmetric three layered (0°/core/0°) square sandwich plates under thermal load

Case A: $\Delta T(x, y, \pm h/2) = T_0 \sin \frac{\pi x}{a} \sin \frac{\pi y}{b}$							
s	Source	$\overline{\sigma_x}\left(\frac{a}{2}, \frac{b}{2}; \pm\frac{h}{2}\right)$	$\overline{\sigma_y}\left(\frac{a}{2}, \frac{b}{2}; \pm\frac{h}{6}\right)$	$10\overline{\tau_{xy}}\left(0, 0, \pm\frac{h}{2}\right)$	$10^2\overline{\tau_{xz}}\left(0, \frac{b}{2}, \pm 0.4h\right)$	$10^2\overline{\tau_{yz}}\left(\frac{a}{2}, 0, \pm 0.4h\right)$	$10^3\overline{w}\left(\frac{a}{2}, \frac{b}{2}, \pm\frac{h}{2}\right)$
4	Present analysis	−0.4505	−0.5315	−3.8640	∓2.4380	∓0.4620	±1.1280
10	Present analysis	−0.0741	−0.0857	−0.6150	∓0.4080	∓0.7610	±0.0260
20	Present analysis	−0.0186	−0.0214	−0.1536	∓0.1026	∓0.0191	±0.0016

Case B: $\Delta T(x, y, h/2) = -\Delta T(x, y, -h/2) = T_0 \sin \frac{\pi x}{a} \sin \frac{\pi y}{b}$							
s	Source	$\overline{\sigma_x}\left(\frac{a}{2}, \frac{b}{2}; \pm\frac{h}{2}\right)$	$\overline{\sigma_y}\left(\frac{a}{2}, \frac{b}{2}; \pm\frac{h}{2}\right)$	$10\overline{\tau_{xy}}\left(0, 0, \pm\frac{h}{2}\right)$	$\overline{\tau_{xz}}\left(0, \frac{b}{2}, \pm 0.4h\right)$	$\overline{\tau_{yz}}\left(\frac{a}{2}, 0, \pm 0.4h\right)$	$10^2\overline{w}\left(\frac{a}{2}, \frac{b}{2}, \pm\frac{h}{2}\right)$
4	Present analysis	±0.6271	∓0.7904	∓2.7440	0.1259	−0.1425	5.6024
10	Present analysis	±0.1317	∓0.1651	∓0.2530	0.0382	−0.0394	0.5139
20	Present analysis	±0.0351	∓0.0441	∓0.0494	0.0109	−0.0111	0.1002

for both cases A and B. Variation of transverse normal stress ($\overline{\sigma_z}$) is seen to be antisymmetric about mid plane (Figure 8b).

Example 4

A symmetric square sandwich plate (0°/core/0°) with simple support end conditions (Table 1) on all four edges and subjected to thermal load has been considered here. Exact solution of this example is not available in the literature. Material properties are presented in Table 3(III). Thickness of each face sheets is one tenth of the total thickness of the plate. The normalized maximum stresses

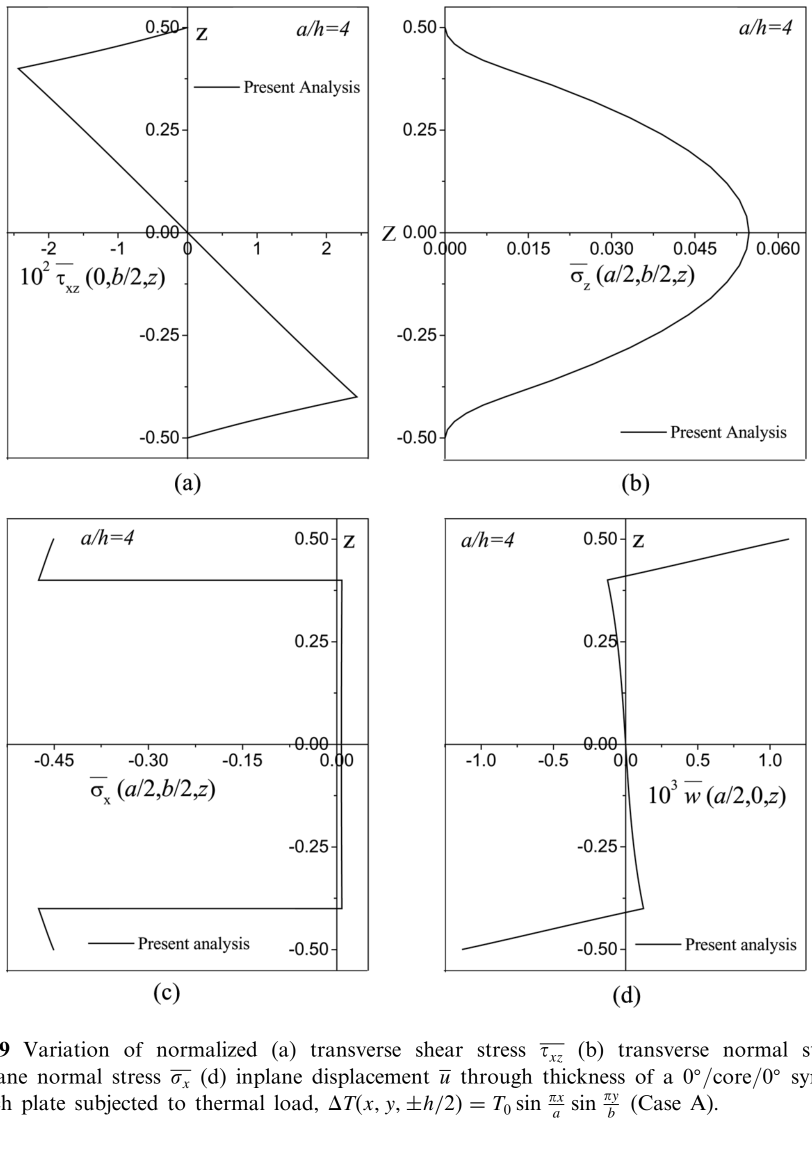

Figure 9 Variation of normalized (a) transverse shear stress $\overline{\tau_{xz}}$ (b) transverse normal stress $\overline{\sigma_z}$ (c) inplane normal stress $\overline{\sigma_x}$ (d) inplane displacement $\overline{u}$ through thickness of a 0°/core/0° symmetric sandwich plate subjected to thermal load, $\Delta T(x, y, \pm h/2) = T_0 \sin\frac{\pi x}{a} \sin\frac{\pi y}{b}$ (Case A).

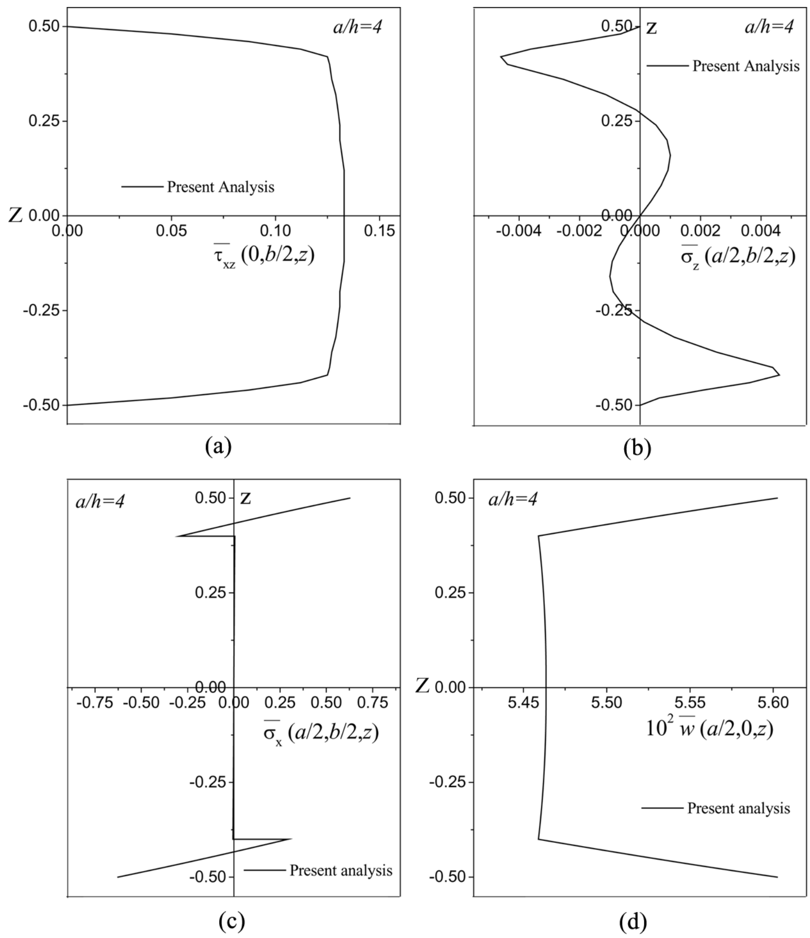

Figure 10 Variation of normalized (a) transverse shear stress $\overline{\tau_{xz}}$ (b) transverse normal stress $\overline{\sigma_z}$ (c) inplane normal stress $\overline{\sigma_x}$ (d) transverse displacement $\overline{w}$ through thickness of a a 0°/core/0° symmetric sandwich subjected to thermal load, $\Delta T(x, y, h/2) = -\Delta T(x, y, -h/2) = T_0 \sin\frac{\pi x}{a} \sin\frac{\pi y}{b}$ (Case B).

$(\overline{\sigma_x}, \overline{\sigma_y}, \overline{\tau_{xy}}, \overline{\tau_{xz}}, \overline{\tau_{yz}})$ and transverse displacement $(\overline{w})$ for various aspect ratios, 4, 10 and 20 are presented in Table 7. Figures 9 and 10 show the through thickness variations of transverse shear stress $(\overline{\tau_{xz}})$, transverse normal stress $(\overline{\sigma_z})$, inplane normal stress $(\overline{\sigma_x})$ and transverse displacement $(\overline{w})$ for an aspect ratio of 4 for case A and case B, respectively. Theses results should serve as benchmark solutions in future.

GENERAL DISCUSSION

The defined variations of temperatures through the thickness of plate are considered here so that present solutions can be compared with the available

3D elasticity results. However, the technique is capable to handle any kind of temperature variations. Further, the present model maintains the continuity of transverse stresses and displacements at the laminae interfaces without involving any complexity in the formulation and solution technique.

It is observed in all examples considered in the present study that variation in transverse displacement ($\overline{w}$) along the thickness is very small for an aspect ratio equal/greater than 10 (thin plate). However, for thick plates with aspect ratios less than 5, $\overline{w}$ varies significantly (Figures 4d, 8d and 10d).

The variation of transverse normal stress ($\overline{\sigma_z}$) here is quite different from what is observed in the case of mechanical loading.

CONCLUDING REMARKS

An efficient, simple semi-analytical model based on solution of a two-point BVP governed by a set of coupled first-order ODEs through the thickness of plate is proposed in this article for thermo-mechanical stress analysis. The shear traction free conditions at the top and bottom of plate and continuity of transverse stresses and displacement at the layer interfaces are exactly satisfied which is one of the important features of the developed model. Moreover, the solution also ensures the fundamental elasticity relationship between stress, strain and displacement fields within the elastic continuum. It is shown through numerical investigations that results obtained by present approach are highly accurate. Another important feature of this approach is that both displacements and stresses are computed simultaneously with the same degree of accuracy.

APPENDIX A

Coefficients of [*C*] Matrix

$$C_{11} = \frac{E_1(1-\nu_{23}\nu_{32})}{\Delta} \quad C_{12} = \frac{E_1(\nu_{21}+\nu_{31}\nu_{23})}{\Delta} \quad C_{13} = \frac{E_1(\nu_{31}+\nu_{21}\nu_{32})}{\Delta}$$
$$C_{22} = \frac{E_2(1-\nu_{13}\nu_{31})}{\Delta} \quad C_{23} = \frac{E_2(\nu_{32}+\nu_{12}\nu_{31})}{\Delta} \quad C_{33} = \frac{E_3(1-\nu_{12}\nu_{21})}{\Delta}$$
$$C_{44} = G_{12} \quad C_{55} = G_{13} \quad C_{66} = G_{23}$$

where $\Delta = (1-\nu_{12}\nu_{21}-\nu_{23}\nu_{32}-\nu_{31}\nu_{13}-2\nu_{12}\nu_{23}\nu_{31})$

APPENDIX B

Coefficients of [*Q*] Matrix

$$Q_{11} = C_{11}c^4 + 2(C_{12}+2C_{44})c^2s^2 + C_{22}s^4$$
$$Q_{12} = C_{12}(c^4+s^4) + (C_{11}+C_{22}-4C_{44})c^2s^2$$
$$Q_{13} = C_{13}c^2 + C_{23}s^2$$

$$Q_{14} = (C_{11} - C_{12} - 2C_{44})c^3s + (C_{12} - C_{22} + 2C_{44})cs^3$$
$$Q_{22} = C_{22}c^4 + 2(C_{12} + 2C_{44})c^2s^2 + C_{11}s^4$$
$$Q_{23} = C_{23}c^2 + C_{13}s^2$$
$$Q_{24} = (C_{12} - C_{22} + 2C_{44})c^3s + (C_{11} - C_{12} - 2C_{44})cs^3$$
$$Q_{33} = C_{33}$$
$$Q_{34} = (C_{31} - C_{32})cs$$
$$Q_{44} = (C_{11} - 2C_{12} + C_{22} - 2C_{44})c^2s^2 + C_{44}(c^4 + s^4)$$
$$Q_{55} = C_{55}c^2 + C_{66}s^2$$
$$Q_{56} = (C_{55} - C_{66})cs$$
$$Q_{66} = C_{55}s^2 + C_{66}c^2$$

APPENDIX C

Coefficients of [*B*] Matrix

$$B_{13} = -\frac{m\pi}{a} \quad B_{14} = \frac{Q_{66}}{Q_{55}Q_{66} - Q_{56}Q_{65}}$$

$$B_{13} = -\frac{n\pi}{b} \quad B_{15} = \frac{Q_{55}}{Q_{55}Q_{66} - Q_{56}Q_{65}}$$

$$B_{31} = \frac{Q_{31}}{Q_{33}}\frac{m\pi}{a} \quad B_{32} = \frac{Q_{32}}{Q_{33}}\frac{n\pi}{b} \quad B_{36} = \frac{1}{Q_{33}}$$

$$B_{41} = \left(Q_{11} - \frac{Q_{13}Q_{31}}{Q_{33}}\right)\frac{m^2\pi^2}{a^2} + \left(Q_{44} - \frac{Q_{43}Q_{34}}{Q_{33}}\right)\frac{n^2\pi^2}{b^2}$$

$$B_{42} = \left[Q_{12} - \left(\frac{Q_{13}Q_{32}}{Q_{33}}\right) - \left(\frac{Q_{43}Q_{34}}{Q_{33}}\right) + Q_{44}\right]\frac{mn\pi^2}{ab} \quad B_{46} = -\left(\frac{Q_{13}}{Q_{33}}\right)\frac{m\pi}{a}$$

$$B_{51} = \left[Q_{21} - \left(\frac{Q_{31}Q_{23}}{Q_{33}}\right) - \left(\frac{Q_{43}Q_{34}}{Q_{33}}\right) + Q_{44}\right]\frac{mn\pi^2}{ab}$$

$$B_{52} = \left(Q_{22} - \frac{Q_{23}Q_{32}}{Q_{33}}\right)\frac{n^2\pi^2}{b^2} + \left(Q_{44} - \frac{Q_{43}Q_{34}}{Q_{33}}\right)\frac{m^2\pi^2}{a^2} \quad B_{56} = -\left(\frac{Q_{23}}{Q_{33}}\right)\frac{n\pi}{b}$$

$$B_{64} = \frac{m\pi}{a} \quad B_{65} = \frac{n\pi}{b}$$

Coefficients of {*p*} Vector

$$p_3 = \frac{1}{Q_{33}}\left(Q_{31}\alpha_{tx} + Q_{32}\alpha_{ty} + Q_{33}\alpha_{tz} + Q_{34}\alpha_{txy}\right)T(z)$$

$$p_4 = -B_x(x, y, z) - \left[\left(-Q_{11} + \frac{Q_{13}Q_{31}}{Q_{33}} \right) \alpha_{tx} + \left(-Q_{12} + \frac{Q_{13}Q_{32}}{Q_{33}} \right) \alpha_{ty} + \left(-Q_{14} + \frac{Q_{13}Q_{34}}{Q_{33}} \right) \alpha_{txy} \right] \frac{m'\pi}{a} T(z)$$

$$p_5 = -B_y(x, y, z) - \left[\left(-Q_{21} + \frac{Q_{23}Q_{31}}{Q_{33}} \right) \alpha_{tx} + \left(-Q_{22} + \frac{Q_{23}Q_{32}}{Q_{33}} \right) \alpha_{ty} + \left(-Q_{24} + \frac{Q_{23}Q_{34}}{Q_{33}} \right) \alpha_{txy} \right] \frac{n'\pi}{b} T(z)$$

$$p_6 = -B_z(x, y, z)$$

REFERENCES

1. V. B. Tungikar and K. M. Rao, Three-Dimensional Exact Solution of Thermal Stresses in Rectangular Composite Laminate, *Composite Structures*, vol. 27, pp. 419–430, 1994.
2. M. Savoia and J. N. Reddy, Three-dimensional Thermal Analysis of Laminated Composite Plates, *Int. J. Solids and Structures*, vol. 32, pp. 593–608, 1995.
3. K. Bhaskar, T. K. Varadan, and J. S. M. Ali, Thermoelastic Solutions for Orthotropic and Anisotropic Composite Laminates, *Composites: Part B*, vol. 27B, pp. 415–420, 1996.
4. J. L. Maulbetsch, Thermal Stresses in Plates, *ASME J. Applied Mechanics*, vol. 57, pp. A141–A146, 1935.
5. W. H. Pell, Thermal Deflection of Anisotropic Thin Plates, *Quart. Appl. Math.*, vol. 4, pp. 27–44, 1946.
6. E. Reissner, The Effect of Transverse Shear Deformation on the Bending of Elastic Plates, *ASME J. Applied Mechanics*, vol. 12, pp. 69–77, 1945.
7. R. D. Mindlin, Influence of Rotatory Inertia and Shear Deformation on Flexural Motions of Isotropic Elastic Plates, *ASME J. Applied Mechanics*, vol. 18, pp. 31–38, 1951.
8. J. N. Reddy and W. C. Chao, Finite Element Analysis of Laminated Bimodulus Composite Material Plates, *Computers and Structures*, vol. 12, pp. 245–251, 1980.
9. F. Weinstein, S. Putter, and Y. Stavsky, Thermoelastic Stress Analysis of Anisotropic Composite Sandwich Plates by Finite Element Method, *Computers and Structures*, vol. 17, pp. 31–36, 1983.
10. R. Rolfes, A. K. Noor, and H. Sparr, Evaluation of Transverse Thermal Stresses in Composite Plates Based on First-order Shear Deformation Theory, *Computer Methods in Applied Mechanics and Engineering*, vol. 167, pp. 355–368, 1998.
11. J. H. Argyris and L. Tenek, High Temperature Bending, Buckling and Postbuckling of Laminated Composite Plates Using the Natural Mode Method, *Computer Methods in Applied Mechanics and Engineering*, vol. 117, pp. 105–142, 1994.
12. T. Kant and R. K. Khare, Finite Element Thermal Stress Analysis of Composite Laminates Using A Higher-order Theory, *J. Thermal Stresses*, vol. 17, pp. 229–255, 1994.
13. A. A. Khdeir and J. N. Reddy, Thermal Stresses and Deflections of Cross-ply Laminated Plates Using Refined Plate Theories, *J. Thermal Stresses*, vol. 14, pp. 419–439, 1991.
14. K. Rohwer, R. Rolfes, and H. Sparr, Higher-order Theories for Thermal Stresses in Layered Plates, *Int. J. Solids and Structures*, vol. 38, pp. 3673–3687, 2001.
15. S. Xioping and S. Liangxin, Thermo-mechanical Buckling of Laminated Composite Plates with Higher Order Transverse Shear Deformation, *Computers and Structures*, vol. 53, pp. 1–7, 1994.

16. J. S. M. Ali, K. Bhaskar, and T. K. Varadan, A New Theory for Accurate Thermal/Mechanical Flexural Analysis of Symmetric Laminated Plates, *Composite Structures*, vol. 45, pp. 227–232, 1999.
17. T. Kant and C. K. Ramesh, Numerical Integration of Linear Boundary Value Problems in Solid Mechanics by Segmentation Method, *Int. J. Numerical Methods in Engineering*, vol. 17, pp. 1233–1256, 1981.
18. R. K. Khare, T. Kant, and A. K. Garg, Closed-form Thermo-mechanical Solutions of Higher-order Theories of Cross-ply Laminated Shallow Shells, *Composite Structures*, vol. 59, pp. 313–340, 2003.